UNWRAPPING METHOD FOR INTERFEROMETRIC IMAGES

Etienne G. Huot *Isaac Cohen* *Isabelle L. Herlin*

INRIA, Rocquencourt, B.P. 105, 78153 Le Chesnay Cedex, France
Etienne.Huot@inria.fr, Isaac.Cohen@inria.fr, Isabelle.Herlin@inria.fr

ABSTRACT

To analyze SAR interferometric data, an unwrapping process must be first performed. Most so far proposed solutions use either local or global methods. In this paper we propose a mixed method to solve this problem, based on a 3-step iterative process: a local unwrapping is first performed and then improved through a markovian segmentation, false unwrapped residues are finally detected and corrected. A deterministic algorithm is used for the relaxation process; wrong unwrapped areas are corrected by a backtracking mechanism. Some results obtained by this approach, which presents a lower computational cost compared to complex stochastic unwrapping methods, are also presented.

1. INTRODUCTION

Since 1986 [1], Interferometric Synthetic Aperture Radar (ISAR) observations provide measures to analyze terrain topography [2] and its small changes with a high accuracy [3, 4]. As for the stereoscopic method, two acquisitions are necessary; each interferogram pixel corresponds to the phase difference between the two radar signals backscattered by the same area. This difference $\Delta\phi$ is theorically linked with the path length difference ΔR ($\Delta\phi \,(\mathrm{mod}\, 2\pi) \simeq \frac{4\pi}{\lambda}\Delta \mathrm{R}$) and is proportional to the elevation of the backscattering cell h (as shown in figure 1).

Since h can be estimated by the phase difference $\Delta\phi = \varphi$ with a modulo 2π ambiguity, unwrapping must be performed to remove it, *ie* to find the right *order* k (label value) verifying $h \propto \Phi = 2\pi k + \varphi$.

There are three main types of unwrapping techniques. First proposed, local methods are based on unwrapping techniques of mono-dimensional signals extended to the bi-dimensional case; for each pixel the order value is chosen according with those of its previously observed neighbors [5, 6]. But with these methods, an error made at one pixel may corrupt the estimated phase values over a large surface. The second category of methods concerns the global approach. It looks for structures, such as edges, to characterize fringes and label them [7, 8]. Usually these methods are less subject to error propagation. Unfortunately these two approaches are very noise sensitive. So, a third approach has been introduced to locally analyze the data with a global effect of the result. Such a method has been proposed by Dupont and *al.* within a markovian framework [9, 10]. However the chosen relaxation algorithm led to a heavy computional cost. In this paper we propose a new method, with a low computational cost and present some associated results.

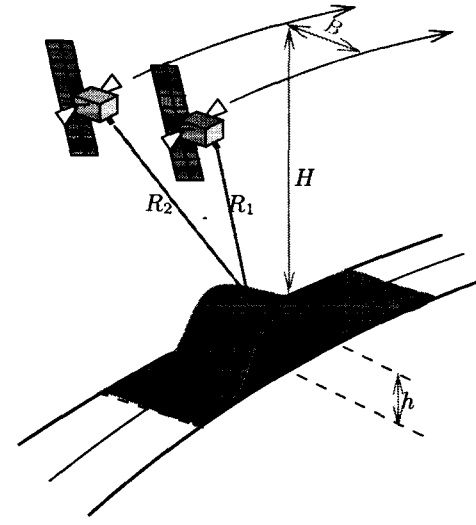

Figure 1. Geometric link between path length difference and elevation h.

2. A MIXED GLOBAL-LOCAL METHOD

Our approach is based on an iterative process: an unwrapping image is first computed with a classical method (described below in step #1), this scene is then improved with a markovian segmentation (step #2), finally residual discontinuities are set as "*not unwrapped*" (step #3) and the process returns to step #1 until an end condition will be satisfied.

2.1. Step #1 – Initialization

The initialization is based on a local method proposed by H. Lim and *al.* [11] where the unwrapping process is performed iteratively:

- for each pixel, a confidence value is computed as the difference between a predicted phase Φ_s^p and the measured one Φ_s:

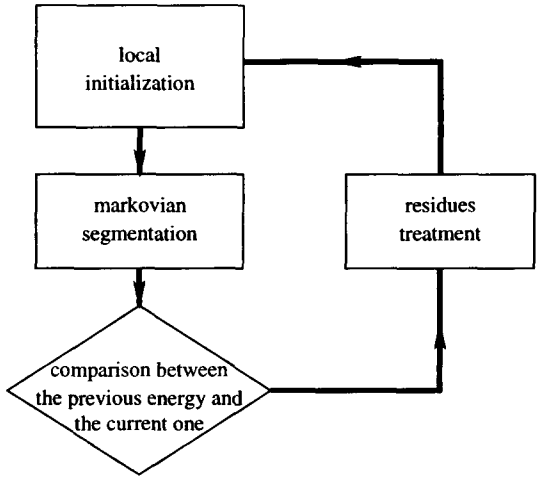

Figure 2. The 3 steps process

- predicted phase: $\Phi_s^p = \dfrac{\sum_{r \in \mathcal{V}_s} w_r \Phi_r}{\sum_{r \in \mathcal{V}_s} w_r}$

  where $\mathcal{V}_s$ is the set of neighbors of the pixel s and w_r is a weight coefficient proportional to the distance between s and its neighbor r;
- measured phase: $\Phi_s = \varphi_s + 2k\pi$

  with k the integer closest to $\dfrac{\Phi_s^p - \varphi_s}{2\pi}$;

- a pixel with low a confidence value that is less than a given threshold is said *reliable*,
- areas with reliable data are unwrapped.

At each step of the iteration, the threshold increases in order to unwrap more pixels. The first lower values used ensure that only reliable unwrapped phase are accepted; the later higher ones, allow more pixels to be unwrapped. This method is fast because the order of each pixel is attributed as soon as the threshold condition is satisfied, and that pixel will never be again examined. However, this is the reason of the hazardous results appearing in case of a low Signal to Noise Ratio (SNR) interferogram. Moreover local errors are often propagated.

2.2. Step #2 – Markovian Segmentation

The second step is a segmentation algorithm performed with a markovian model [12]. The previously unwrapped interferogram is considered like a system, and an energy function is defined on a neighborhood system with associated potential functions. The system solution is reached when the energy is minimum.

Let:

- S be the set of image pixels,
- $K = (K_s)_{s \in S} \in \Omega = \{1..k_{max}\}^{|S|}$ the segmentation process corresponding to the order,

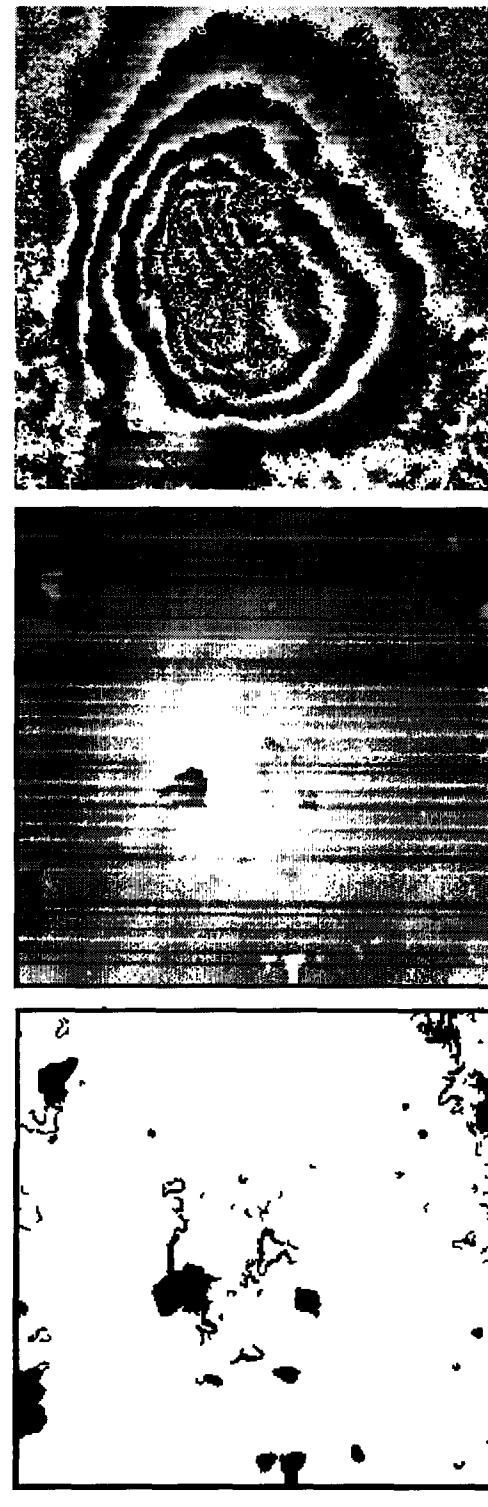

Figure 3. Up: Mount Etna interferogram. Center: Unwrapped phase after one iteration of the process (step #1 and #2). Down: Residue image (step #3).

- $\Psi = (\Psi_s)_{s \in S} \in \Delta = [0..2\pi]^{|S|}$ the random variable used to describe the phase, corresponding to the grey level value of the interferogram,
- $k = (k_s)_{s \in S}$ and $\varphi = (\varphi_s)_{s \in S}$ are respectively the values of the random variables K and Ψ.

We are given a Markov Random Field on these pixel sites, defined by a neighborhood system $\mathcal{V} = \{\mathcal{V}_s, s \in S\}$, where $\mathcal{V}_s$ is the set of neighbors of the pixel s, and by clique potentials.

Like most models we use a first energy term based on a membrane model:

$$U_1(\varphi, k) = \sum_{s \in S} \sum_{r \in \mathcal{V}_s} |(\varphi_s + 2k_s\pi) - (\varphi_r + 2k_r\pi)|$$

U_1 measures the reconstructed surface regularity.

We add a second term based on the local homogeneity within a fringe according to a small neighborhood (a pixel tends to have the same order than its neighbor with the closest grey level value):

$$U_2(\varphi, k) = \sum_{s \in S} \frac{\sum_{r \in \mathcal{V}_s} |\varphi_s - \varphi_r| \chi(k_s = k_r)}{\sum_{r \in \mathcal{V}_s} \chi(k_s = k_r)}$$

where $\chi(k_s = k_r) = 1$ if $k_s = k_r$ and 0 otherwise. U_2 measures the local phase homogeneity.

The optimal labeling is obtained with a deterministic optimization method (Iterated Conditional Mode). The result of step #1 is used to start this relaxation algorithm.

2.3. Step #3 – Residues

Due to the deterministic relaxation, the result often corresponds to a local minimum, presenting discontinuities, *ie* regions where the phase difference between two neighbors is greater than π. To reduce these discontinuities, we classify them as "residues" labeled to "*not even unwrapped*".

Then we iterate the global unwrapping process and return to step #1.

The global iteration process ends when the energy value becomes stable in step #2 (see figure 4).

3. RESULTS

The data interferogram and the result of the method with one iteration of the global unwrapping process are displayed in figure 3. The result after eight iterations may be seen on figure 5.

The main advantage of this method is the use of the local properties of the markovian approach without its usual heavy computational cost. The result is obtained the with about 10 iterations of the global unwrapping process and less than 200 iterations for each ICM (step #2), versus 2,000 to 100,000 iterations in the stochastic optimization case. As the gray arrows shows in figure 5, this method allows some true discontinuities (the pointed one is due to the radar incidence). Furthermore, all pixels are always unwrapped, *ie* no pixel will be labeled as unwrappable. This can be interesting for areas with a low SNR, like the top of mount Etna. However, in areas with no coherence, the obtained labels will be meaningless: the Ionic sea surface pointed by the black arrow on figure 5 should be a flat area.

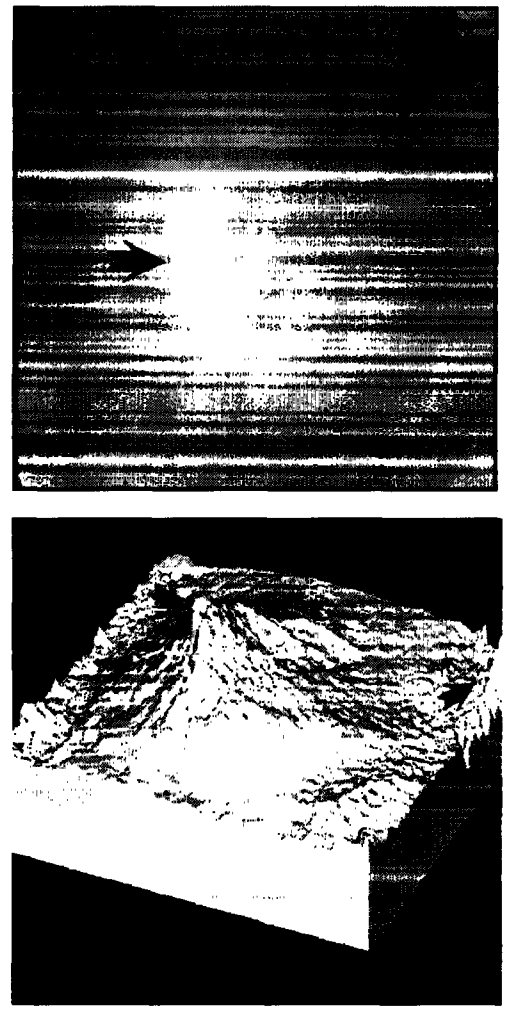

Figure 5. The final unwrapped image and the reconstructed DEM.

4. PERSPECTIVES

Two types of discontinuities may occur within the unwrapping process: discontinuities caused by initialization errors or true ground discontinuities. The first one must be corrected but the second must be keeped. This could be achieved by classifying the true and false discontinuities. For example we could make use of a segmentation technique like that proposed by E. Trouvé and *al.* [13] where unwrapping obstacles are detected through a classification merging several measures performed over the phase, coherence and amplitude data. An alternative could be the use of these coherence and amplitude images to compute another potential function allowing true discontinuities.

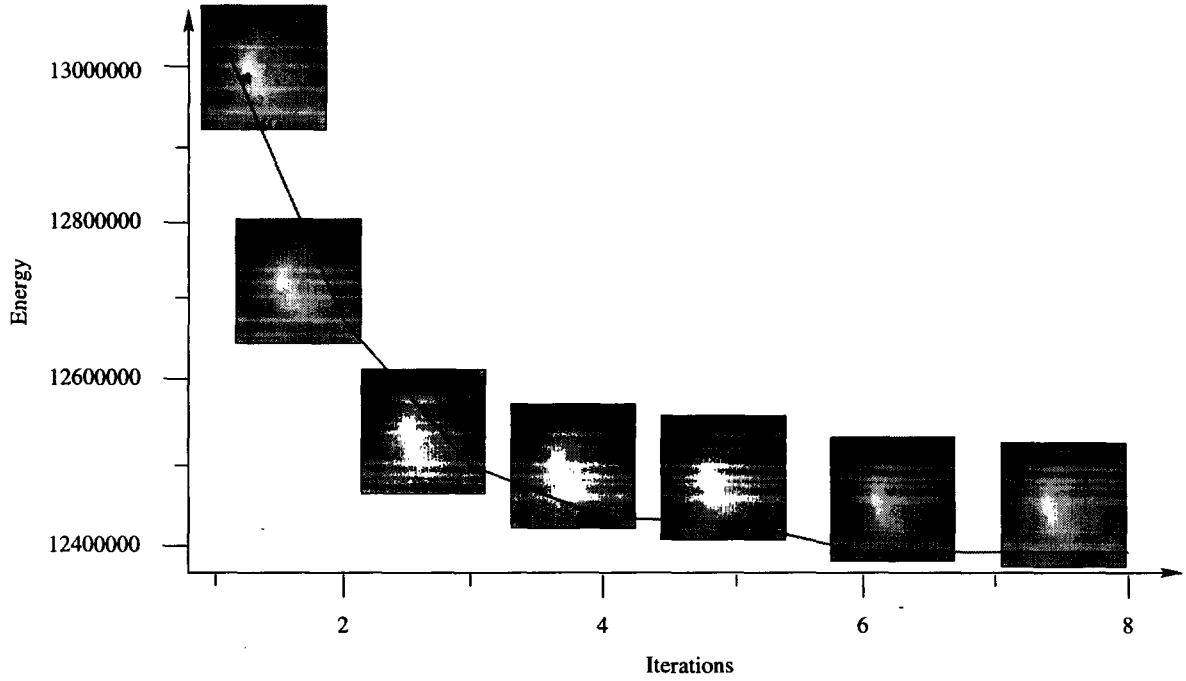

Figure 4. Global energy variation during the eight iterations of the unwrapping process of the Etna interferogram.

ACKNOWLEDGMENTS

We thank CNES and Matra Cap Système companies for providing us ERS-1 and SIR-B interferograms.

REFERENCES

[1] H. Zebker and R. Goldstein. Topographic mapping from interferometric SAR observations. *Journal of Geophysic Research Science*, 91(B5), April 1986.

[2] C. Prati and Rocca. Limits to the resolution of elevation maps from stereo sar images. *International Journal of Remote Sensing*, 11(12):2215–2216, 1990.

[3] D. Massonnet. Giving an operational status to SAR interferometry. In *First ERS-1 Pilot Project Workshop*, pages 379–382, Toledo, Spain, June 1994.

[4] D. Massonnet and T. Rabaute. Radar interferometry: Limits and potential. In *IEEE Transactions on Geoscience and Remote Sensing*, volume 31, pages 455–464, March 1993.

[5] R. Goldstein, H. Zebker, and C. Werner. Satellite radar interferometry: two dimensional phase unwrapping. *Radio Science*, (4), July 1988.

[6] C. Prati, F. Rocca, A. M. Guarinieri, and E. Damonti. Seismic migration for SAR focusing interferometrical applications. In *IEEE Trans. on Geoscience and Remote Sensing*, volume 28, pages 627–640, July 1990.

[7] Q. Lin, J. F. Vesecky, and H. Zebker. New approach in interferometric SAR data processing. In *IEEE Trans. on Geoscience and Remote Sensing*, volume 30, No 3, May 1992.

[8] F. Perlant and D. Massonnet. Different SPOT DEM applications for studies in SAR interferometry. In *XVII ISPRS Congress, Commission IV*, volume XXIX, pages 87–93, 1991.

[9] S. Dupont, D. Labrousse, and M. Berthod. SAR interferometry: an application of simulated annealing to phase unwrapping. In *SCIA'95*, Upsala, Sweden, June 1995.

[10] D. Labrousse, S. Dupont, and M. Berthod. SAR interferometry: a markovian method to phase unwrapping. In *AeroSense, Integrating Photogrametric Techniques with Scene Analysis and Machine Vision II*, Orlando, Florida, USA, April 1995.

[11] Hock Lim, Wei Xu, and Xiaojing Huang. Two new practical methods for phase unwrapping. In *IGARSS'95*, April 1995.

[12] S. Geman and D. Geman. Stochastic relaxation, Gibbs distributions and the Bayesian restoration of images. In *IEEE Trans. Pattern Anal. Machine Intell*, volume 6, No 6, pages 721–741, 1984.

[13] E. Trouvé, M. Caramma, and H. Maître. Analyse et restoration de phase interferométrique en radar à ouverture de synthèse. In *GRETSI'95*, volume 1, pages 501–504, Juan-les-Pins, France, 1995.